

Cardiotoxicity Evaluation of Tyrosine Kinase Inhibitors using Human Induced Pluripotent Stem Cell-derived Healthy and Long QT Syndrome Cardiomyocytes

Yizhe Zhang

China State Institute of Pharmaceutical Industry, Shanghai InnoStar Bio-Tech Co.,Ltd

Meiting Wang

China State Institute of Pharmaceutical Industry, Shanghai InnoStar Bio-Tech Co., Ltd

Qi Zhao

Shanghai InnoStar Bio-Tech Co., Ltd

Hongyan Xing

Shanghai InnoStar Bio-Tech Co., Ltd

Xin Yang

China State Institute of Pharmaceutical Industry, Shanghai InnoStar Bio-Tech Co., Ltd

Xijie Wang (✉ xjwang@ncdser.com)

Research

Keywords: hiPSC-CMs, LQT, cardiotoxicity, RTCA cardio system, tyrosine kinase inhibitor

Posted Date: May 14th, 2020

DOI: <https://doi.org/10.21203/rs.3.rs-27568/v1>

License:  This work is licensed under a Creative Commons Attribution 4.0 International License.

[Read Full License](#)

Abstract

Background

Cardiotoxicity associated with tyrosine kinase inhibitors (TKIs) has been reported in several clinical trials and preclinical studies, whereas the toxicity in populations with congenital electrophysiological dysfunction remains unclarified.

Methods

We studied cardiotoxicities of four US Food and Drug Administration (FDA)-approved TKIs with different targets by measuring changes in cardiomyocyte (CM) contractility. Contractions of human induced pluripotent stem cell-derived (hiPSC)-CMs from healthy donors and long QT syndrome (LQT) patients were studied with an impedance-based bioanalytical method (xCELLigence® real-time cell analysis [RTCA] cardio system) to quantify TKI toxicity.

Results

Both healthy donor (wild type, WT)- and LQT patient-derived hiPSC-CMs exhibited a functional CM phenotype. The four TKIs inhibited the growth and contractility of CMs with different potencies. Crizotinib and dasatinib decreased the beating of both WT- and LQT-hiPSC-CMs with approximately equal potencies. Sunitinib weakened spontaneous pulsations of both kinds of cells, but the LQT-hiPSC-CMs showed higher sensitivity. In contrast, lapatinib exerted a milder effect on LQT- hiPSC-CMs.

Conclusions

Crizotinib, sunitinib, and lapatinib have a higher risk of inducing adverse cardiac events than dasatinib, and LQT1 patients should be particularly cautious with sunitinib. HiPSC-CMs derived from both healthy and patient-specific donors could improve precision medicine and preclinical cardiotoxicity evaluations.

Background

The clinical application of molecular-targeted tyrosine kinase inhibitors (TKIs) has revolutionized the treatment of cancer; however, cardiovascular toxicities are frequent critical issues in patients administered these drugs [1]. Cardiotoxicities of TKIs vary and common manifestations include cardiac dysfunction, arrhythmias, and vascular and pericardial diseases. Current research suggests that TKIs target receptors and cytoplasmic kinases [2]. Both “on-target” and “off-target” effects of these agents could cause organ-specific toxicity [3]. Therefore, preclinical evaluation of cardiotoxicity is important in the evaluation of novel TKIs.

However, certain adverse reactions are unexpected and cannot be accurately predicted from previous standard preclinical studies. To date, several preclinical approaches have been used to test the cardiotoxicity of compounds, such as using hearts-on-chips, engineered heart tissue models, and the most widely used, human induced pluripotent stem cell-derived cardiac myocytes (hiPSC-CMs). Particularly, hiPSC-CMs have provided a new platform for building *in vitro* models that have been widely used in activities such as disease modeling, drug development and screening, and evaluation of cardiotoxicity. Compared with animal models, hiPSC-CMs have no species and extrapolation limitations. In addition, in contrast to non-cardiac human cell lines, hiPSC-CMs express the native cardiac proteins required to reconstitute the complex cardiac structure and phenotype (e.g., sarcomere organization, calcium handling, metabolism, and electrophysiology) [4].

Based on these characteristics, patient-derived cardiomyocytes (CMs) contribute to the understanding of mechanisms underlying genetic diseases and enable the study of differences between a drug's activity in healthy and particular patient groups [5, 6]. Differential patient-specific reactions to a particular drug are driven by interactions between genetic, epigenetic, and environmental factors, and drug pharmacodynamics could also be influenced by inherited polymorphisms in target enzymes, transporters, ion channels, and receptors [7]. Multiple patient-specific hiPSC-CMs have been established successfully and used in studies of pathogenic pharmacodynamic mechanisms and compound screening [8, 9]. For instance, patient-specific (long QT syndrome 1 [LQT1] and LQT2) CMs have been used to explore cardioactive drug effects, and the results appear to indicate that these cells simulate clinical observations (4). These studies provide further evidence to support the notion that these cells can be used to evaluate the arrhythmia-inducing propensity of drugs [10].

LQT is an inherited arrhythmia syndrome, which manifests as palpitations, syncope, sudden cardiac death, and clinical susceptibility to malignant ventricular arrhythmias. LQT is always associated with sudden cardiac death caused by torsade de pointes (TdP). The electrocardiogram (ECG) indicators of LQT are prolonged QT intervals and increased QT dispersion. Inherited forms of LQTs are caused by mutations in cardiac ion channel coding genes. The potassium voltage-gated channel subfamily Q member 1 (*KCNQ1*, LQT1), potassium voltage-gated channel subfamily H member 2 (*KCNH2*, LQT2), and sodium voltage-gated channel alpha subunit 5 (*SCN5A*, LQT3) are the most common LQT pathogenic genes, and LQT1 is the most common inherited LQT.

Mutation of the *KCNQ1* gene reduces the main component of the cardiac repolarization outward current, the slow delayed rectifier current (I_{Ks}) channel, which delays ventricular repolarization and QT interval extension. The I_{Ks} channel has two major components: KCNQ1 (also called $K_v7.1$ or K_v LQT1, the major ion-conducting, voltage-sensing component) and potassium voltage-gated channel subfamily E regulatory subunit 1 (*KCNE1*, also known as minK or I_{sK} , a small regulatory subunit). In the human heart, I_{Ks} is mainly responsible for shortening ventricular action potentials under stressful conditions such as with high β -adrenergic tone.

Therefore, adverse cardiac events in LQT1 patients occur mostly during exercise or under emotional stress [11]. To date, over 250 *KCNQ1* mutations have been found linked to LQT1 and new mutations continue to be identified. Mutations in the transmembrane, linker, and pore regions of *KCNQ1* are usually defined as high-probability, disease-causing mutations that tend to cause severe cardiac events in patients at a younger age than mutations in the C-terminal region [12].

The numerous adverse cardiac events associated with TKIs have raised the question whether patient groups with existing ion channel dysfunction have similar susceptibility to TKI cardiotoxicity. Drug-induced cardiotoxicity usually manifests clinically as contractile dysfunction. The xCELLigence® real-time cell analysis (RTCA) cardio system, which utilizes impedance technology to quantify CM-beating properties, has been previously reported as an emerging method to quantify cardiac contractility [13]. In the present study, to the best of our knowledge this is the first time, we compared the responses of healthy and LQT1 CMs to TKIs with different targets using healthy donor (wild type, WT)- and LQT syndrome patient-derived hiPSC-CMs, with the aim of providing a reference for the appropriate clinical drug treatment of particular patient groups.

Methods

Chemicals

Four TKIs were investigated: crizotinib, dasatinib, lapatinib (all from Sigma-Aldrich, St. Louis, MO, USA; PZ0191, CDS023389, and CDS022971, respectively), and sunitinib (Aladdin, Shanghai, China; S126061). The TKIs were dissolved in dimethyl sulfoxide (Sigma-Aldrich, D4540) and the diluted drugs were equilibrated in a 37 °C, 5% CO₂ incubator for 30 min before being applied to the cells.

Cell culture

WT-hiPSC-CMs and LQT-hiPSC-CMs were purchased from Cellapy (CA2101106, Beijing, China) and HELP (HELP4120, Nanjing, China), respectively. Both cell types were obtained as frozen 1 mL aliquots containing approximately 1 and 2 million cells, respectively. The cells were thawed and plated in 96-well E-plates (ACEA Biosciences, Hangzhou, China) pre-coated with 0.1% gelatin. The cells were incubated in maintenance medium at 37 °C in an atmosphere of 5% CO₂, and the culture medium was refreshed every 2 days. The WT and LQT cells were plated at densities of 3×10^4 and 6×10^4 cells/well, respectively.

Clinical data

The somatic cells for generation of the WT-hiPSC-CMs were obtained from a 39-year-old healthy female volunteer in Beijing by Cellapy, while those for the LQT1-hiPSC-CMs were from a 53-year-old Uyghur female patient with LQTS1 by HELP. The patient's LQTS1 was due to an identified missense mutation (G to A substitution at nucleotide 656), resulting in an amino acid substitution at position 219 of glycine to glutamic acid (G219E) in the *KCNQ1* channel.

Real-time impedance-based bioanalyses of hiPSC-derived CMs

Spontaneous CM contraction and cell health were monitored in real-time by impedance using the xCELLigence® RTCA cardio system (ACEA Biosciences, Hangzhou, China). Impedance signals were monitored and recorded for 20 s per sweep. The cell index (CI), which is related to cell adherence and growth, was used as a measure of cell vitality.

Data and statistical analyses

For RTCA CM monitoring, the CI, beating rate, beating amplitude, and half-maximal inhibitory concentration (IC_{50}) for each well were calculated off-line using RTCA cardio software 1.0 and normalized to the corresponding baseline values measured prior to treatment with the compounds. A threshold level of 12 was used to suppress noise for improved peak recognition and the raw data of the beat curves were displayed using a threshold level of 0. The data are presented as means \pm standard error of the mean (SEM) and the statistical significance of differences was estimated using a one-way analysis of variance (ANOVA) or Student's *t* test. A value of $p < 0.05$ was considered significant.

Results

WT- and LQT-hiPSC-CMs exhibit functional CM phenotypes in culture

Analysis of the hiPSC-CMs based on marker protein expression and electrophysiological measurements revealed that the expected phenotypes were replicated in these cell models, namely that the WT-hiPSC-CMs had a normal phenotype and the LQT-hiPSC-CMs showed QT-interval prolongation. The relevant certificate of analysis is provided in the Supplementary data. Spontaneously contracting CMs were observed in both WT- and LQT-hiPSC-CMs as assessed by light microscopy.

The CI values increased and gradually stabilized with the growth and adherence of both WT- and LQT-hiPSC-CMs (Fig. 1a and 1c). Within 168 h after plating, the WT-hiPSC-CMs achieved a stable state in both beating rate and amplitude earlier than the LQT-hiPSC-CMs did (Fig. 1b and 1d, Fig. 2a and 2b). The spontaneous beating rate of both WT- and LQT-hiPSC-CMs was stable at approximately 40 bpm, and the amplitude steadily increased over time and stabilized at approximately 0.09, with a rhythmic irregularity $< 40\%$ (Fig. 2c).

Effects of drugs on WT- and LQT-hiPSC-CMs

Effects of crizotinib

Crizotinib reduced the CI of both WT- and LQT-hiPSC-CMs in a concentration-dependent manner, indicating its inhibitory effect on the growth and adherence of cells at concentrations $> 3 \mu\text{mol/L}$ (Fig. 3a and 3b). In addition, 3 $\mu\text{mol/L}$ and 10 $\mu\text{mol/L}$ crizotinib abolished the cellular automaticity of both WT- and LQT-hiPSC-CMs, but the latter CMs showed signs of recovery (Fig. 3c and 3d). Further analysis of the beating rate indicated that crizotinib inhibited WT- and LQT-hiPSC-CMs in a concentration-dependent manner. The beating rate was reduced at concentrations $> 0.1 \mu\text{mol/L}$, and the spontaneous pulsations gradually recovered over time (Fig. 3e and 3 g). In contrast, a detailed trace analysis revealed that 0.3 $\mu\text{mol/L}$ and 1 $\mu\text{mol/L}$ increased the amplitude of both WT- and LQT-hiPSC-CMs (Fig. 3f and 3 h). While spontaneous beating ceased early after administration of crizotinib, the amplitude significantly increased after beating was restored. Analysis of the concentration-related effects of crizotinib on WT- and LQT-hiPSC-CMs demonstrated IC₅₀ values of 0.89 $\mu\text{mol/L}$ and 0.76 $\mu\text{mol/L}$, respectively (Table 1).

Table 1

Comparison of wild-type (WT)- and long QT syndrome (LQT)-human induced pluripotent stem cell-derived cardiomyocytes (hiPSC-CMs)

TKI	IC ₅₀ ($\mu\text{mol/L}$)		C _{max} ($\mu\text{mol/L}$) [35]
	WT-hiPSC-CMs	LQT-hiPSC-CMs	
Crizotinib	0.89	0.76	1.24
Sunitinib	4.71	0.52	0.18
Dasatinib	27.34	23.30	0.21
Lapatinib	6.87	10.89	2.30

TKI: tyrosine kinase inhibitor, IC₅₀: half-maximal inhibitory concentration, C_{max}: maximum serum concentration

Effects of sunitinib

Investigation of the effects of sunitinib demonstrated that it decreased the CI of WT-hiPSC-CMs in a concentration-dependent manner (Fig. 4a). Sunitinib at a concentration of 3 $\mu\text{mol/L}$ affected pulse signals, while 10 $\mu\text{mol/L}$ entirely abolished spontaneous beating (Fig. 4c). Thirty minutes after administration, the spontaneous beating rhythms of WT-hiPSC-CMs were markedly decreased at 1 $\mu\text{mol/L}$ and 3 $\mu\text{mol/L}$ in a concentration-dependent manner without self-recovery within the observation period (Fig. 4e). Similarly, sunitinib at 1 $\mu\text{mol/L}$ and 3 $\mu\text{mol/L}$ increased the beating amplitude 0.5 h after administration, but a gradual recovery was observed over time (Fig. 4f). In the LQT-hiPSC-CMs, sunitinib reduced the CI values in a concentration-dependent manner. However, compared with the WT-hiPSC-CMs at the highest concentration (10 $\mu\text{mol/L}$), sunitinib reduced CI values to 0 within approximately 0.5 h, which indicates that this concentration completely inhibited cell growth (Fig. 4b). Likewise, for pulse patterns, the LQT-hiPSC-CMs showed a higher sensitivity to sunitinib than the WT-hiPSC-CMs did, where sunitinib weakened pulse signals at concentrations $\geq 0.3 \mu\text{mol/L}$ in the former (Fig. 4d). Further analysis demonstrated that sunitinib decreased the beating rate and amplitude of the LQT-hiPSC-CMs in a

concentration-dependent manner, and a gradual recovery was observed up to 6 h after exposure (Fig. 4g and 4 h). Interestingly, the LQT-hiPSC-CMs showed weak beating at a lower concentration (0.3 μ mol/L) of sunitinib than the WT-hiPSC-CMs did. Evaluation of the concentration-dependent effects of sunitinib on WT- and LQT-hiPSC-CMs demonstrated IC₅₀ values of 4.71 μ mol/L and 0.52 μ mol/L, respectively (Table 1).

Effects of dasatinib

Dasatinib reduced the CI values (Fig. 5a and 5b) and affected the pulse patterns (Fig. 5c and 5d) of both WT- and LQT-hiPSC-CMs in a concentration-dependent manner. In the WT-hiPSC-CMs, 30 μ mol/L dasatinib affected pulse patterns, which was observed as inhomogeneity in the pulse rhythm and amplitude (Fig. 5c). Analysis of the beating rate and amplitude within 24 h after exposure indicated that dasatinib concentration-dependently inhibited the beating rate at $\geq 3 \mu$ mol/L 0.5 h after exposure (Fig. 5e). In contrast, the effect of dasatinib was relatively milder on the beating amplitude than it was on the beating rate. Furthermore, at the highest concentration (30 μ mol/L), dasatinib increased the cell amplitude (Fig. 5f). In the LQT-hiPSC-CMs, dasatinib affected pulse patterns at 10 μ mol/L and 30 μ mol/L, and 30 μ mol/L dasatinib temporarily interrupted spontaneous beating 0.5 h after exposure (Fig. 5d). Lower concentrations (0.3 μ mol/L and 3 μ mol/L) of dasatinib temporary increased the beating rate of LQT-hiPSC-CMs 0.5 h after exposure, but the cells soon recovered (Fig. 5g). However, 10 μ mol/L and 30 μ mol/L dasatinib exerted remarkable inhibitory effects on the beating rate without self-recovery within 24 h after exposure. Consistently, in the LQT-hiPSC-CMs, dasatinib affected the beating amplitude less than it did the beating rate, and with the highest concentration (30 μ mol/L), the beating amplitude increased after recovery of spontaneous beating (Fig. 5h). Evaluation of the concentration-dependent effects of dasatinib on WT- and LQT-hiPSC-CMs demonstrated IC₅₀ values of 27.34 μ mol/L and 23.30 μ mol/L, respectively (Table 1).

Effects of lapatinib

Investigations of the effects of lapatinib on the WT-hiPSC-CMs demonstrated that it reduced CI values in a concentration-dependent manner (Fig. 6a), and interrupted pulse signals at concentrations $\geq 10 \mu$ mol/L (Fig. 6c). In this study, lapatinib exerted a mild inhibitory effect on the beating rate and amplitude of WT-hiPSC-CMs at 1 μ mol/L and 3 μ mol/L, and self-recovery was observed within the study period. However, at 10 μ mol/L and 30 μ mol/L, lapatinib totally abolished the beating of WT-hiPSC-CMs without recovery (Fig. 6e and 6f). Furthermore, a concentration-dependent inhibition of CI values for the LQT-hiPSC-CMs was observed at $\geq 10 \mu$ mol/L (Fig. 6b), and beating of the cells in some wells was arrested from 1 h to 12 h at 10 μ mol/L. In addition, the cells in all wells treated with 30 μ mol/L ceased beating within 24 h after exposure (Fig. 6d). Further analysis showed that lapatinib at lower concentration (0.3 μ mol/L to 3 μ mol/L) increased the beating rate of LQT-hiPSC-CMs minimally, while 10 μ mol/L markedly decreased the rate and even stopped the beating early after exposure (Fig. 6g). In addition, lapatinib exerted a concentration-dependent inhibitory effect on the beating amplitude of the LQT-hiPSC-CMs (Fig. 6h).

Evaluation of the concentration-dependent effects of lapatinib on WT- and LQT-hiPSC-CMs demonstrated IC₅₀ values of 6.87 μmol/L and 10.89 μmol/L, respectively (Table 1).

Discussion

TKI-induced cardiotoxicity remains a major consideration in the treatment of cancer. In this study, using a stem cell-based strategy, we compared the beating parameters of CMs derived from a healthy donor and LQT1 patient before and after exposure to TKIs. Our results demonstrated that hiPSC-CMs simulate many physiological characteristics of human CMs, which is consistent with the increasing use of hiPSC-CMs as potential *in vitro* models for identifying drug targets as well as determining drug responses and toxicities.

In the current study, before exposure to different TKIs, the spontaneous beating rate of both WT- and LQT-hiPSC-CMs was stable at approximately 40 bpm. Paci et al. [14] demonstrated that the rate of spontaneous beating of ventricular- and atrial-like hiPSC-CMs was 35.3 ± 2.2 and 50 ± 10, respectively, by developing two computational models of hiPSC-CM action potential. This previously published result supports our finding and indicates that the CMs we studied likely exhibited a ventricular-like phenotype. Another *in silico* model based on hiPSC-CMs was able to reproduce the LQT syndrome with large-scale simulations, and this LQT1 model showed a beating rate of 44 ± 14 [15], similar to the results of our study. After stabilizing the cells in our study, they were treated with different TKIs to determine the sensitivity of the two types of CM models to these agents.

Crizotinib, a receptor TKI with several targets including c-ros oncogene1 (ROS1) and MET protooncogene (MET), is mainly used to treat anaplastic lymphoma kinase (ALK)-positive advanced non-small cell lung cancer (NSCLC). The most frequent crizotinib-related cardiotoxicities reported in clinical trials were QT interval prolongation and bradycardia [16, 17]. Consistent with these clinical findings, slowing of the beating rate was observed in our study, and both WT- and LQT-hiPSC-CMs lost all synchronous contractions 0.5 h after treatment with 3 μmol/L crizotinib.

Similarly, Doherty et al. [18] evaluated the cardiotoxicity of crizotinib and discovered that the cessation of beating induced by 10 μmol/L crizotinib lasted for up to 24 h. Our results indicated that WT- and LQT-hiPSC-CMs exhibited a similar sensitivity to crizotinib. Previous studies considered that the pathogenesis of crizotinib-induced bradycardia is probably related to the drug's antagonism of L-type calcium channels, chronotropic effects on the sinoatrial node, anti-mesenchymal-epithelial transition effects, or anti-MET effects [19, 20]. Moreover, crizotinib could affect other ion channels, and it was shown to block human ether-a-go-go-related gene (hERG) and Na_v1.5 ion channels with IC₅₀ values of 1.7 μmol/L and 3.5 μmol/L, respectively.

In addition to blockade of ion channels, reactive oxygen species (ROS) accumulation, activation of the apoptotic cascade, and increased cholesterol synthesis contribute to the cardiotoxicity of these drugs [18]. Therefore, the cardiotoxicity of crizotinib does not seem to involve the I_{Ks}, but is likely related to

inhibition of Ca_v ion channels and metabolism. The multi-ion channel inhibition suggests that LQT1 patients do not necessarily have higher sensitivity to cardiotoxicities than non-LQT1 patients.

Sunitinib targets vascular epidermal growth factor receptor 1 (VEGFR1)-3, platelet-derived growth factor receptor (PDGFR)- α and - β , and colony-stimulating factor 1 receptor (CSF1R) [19]. This agent is known for its therapeutic effect on renal cell carcinoma, chronic myeloid leukemia, imatinib-resistant gastrointestinal stromal tumor, pancreatic cancer, and neuroendocrine tumors [2]. The cardiotoxicity of sunitinib has been reported in several clinical trials and it causes hypertension and myocardial ischemia frequently because it inhibits blood circulation.

In the cardiovascular system, the tyrosine kinase inhibition induced by sunitinib impairs cellular signal transduction, cell cycle regulation and metabolism, and transcription [21]. In our study, 10 $\mu\text{mol/L}$ sunitinib potently affected the growth of both WT-hiPSC-CMs and LQT-hiPSC-CMs. Previous studies have illustrated the major pathways mediating the toxicity of sunitinib, including inhibition of VEGF and PDGFR signaling and coronary microvascular dysfunction [20]. Activation of the endothelin-1 system, inhibition of stem cell growth factor receptor, and cellular energy compromise due to inhibition of AMP-activated protein kinase (AMPK) also contribute to progression of the toxicity of sunitinib [21].

Therefore, the negative effect of sunitinib on the overall survival rate of CMs is mainly mediated by activation of apoptotic pathways and disruption of energy metabolism. Moreover, LQT-hiPSC-CMs exhibited a more severe dysfunction of spontaneous beating. A previous study indicated that sunitinib blocked the hERG channel but had less effect on $\text{Na}_v1.5$ and Ca_v ion channels, which possibly explains the aggravated burden of repolarization in LQT patients [18]. These results suggest that LQT1 patients should be more closely monitored under such treatments.

Dasatinib was approved by the US Food and Drug Administration (FDA) in 2006 as a small-molecule BCR-ABL1-targeted TKI. Thus, this agent was first used to treat patients with Philadelphia chromosome positive (Ph^+) chronic myeloid leukemia (CML) in the chronic accelerated and acute phases, who were intolerant or resistant to imatinib. Cardiovascular toxicities including pleural effusions, pulmonary arterial hypertension, and QT interval prolongation can occur during treatment with dasatinib.

Compared to other TKIs, dasatinib is thought to have relatively few cardiac side effects because the mean QT interval change is only 3–13 ms [22]. In agreement with this notion, in this study, the CMs were less affected at the highest concentration (10 $\mu\text{mol/L}$) of dasatinib than with the other tested TKIs. However, the risk of reduction in heart rate cannot be ignored, particularly with LQT1 patients. The spontaneous beating rate was inhibited in a concentration-dependent manner to the same degree in both CM models, and the amplitude showed a compensatory increase. Although temporary cessation of beating occurred in the LQT-hiPSC-CMs 0.5 h after exposure, the amplitude still showed an increasing trend.

Recently, a study indicated that dasatinib decreased heart rate and cardiac output in a dose-dependent manner, and cardiac troponin I levels were also increased *in vivo* in treated dogs [23, 24]. These results

indicate that minor myocardial damage caused by dasatinib and mitochondrial dysfunction might be the most plausible explanations for the observed results. Moreover, dasatinib had a stronger effect on the contraction rate than it did on the amplitude, which could explain the negative inotropic effect observed *in vivo*.

Lapatinib targets human epidermal growth factor receptor 2 (HER2, HER2/neu, or ErbB2) and epidermal growth factor receptor (EGFR)/HER1 and is used in combination with capecitabine for the treatment of ErbB2 overexpression in advanced or metastatic breast cancers [25]. The most common clinical manifestation of the cardiotoxicity of lapatinib is decreased left ventricular ejection fraction (LVEF), although the underlying mechanism is still not completely understood [26]. Likewise, in our study, lapatinib decreased the spontaneous beating at a notably lower concentration than the other TKIs and caused beating cessation at $\geq 10 \mu\text{mol/L}$. However, in the LQT-hiPSC-CMs, we observed an increased rate at lower concentrations. The amplitude from the LQT-hiPSC-CMs was decreased in a lapatinib concentration-dependent manner. Recently, it was reported that lapatinib suppressed I_{K_s} , I_{K_r} , and I_{K_1} , but not I_{Ca} , and suppressed the amplitude of peak I_{Na} , with IC_{50} values of $1.84 \mu\text{mol/L}$ and $0.8 \mu\text{mol/L}$, against I_{K_s} and I_{K_r} , respectively. Furthermore, the QTc (corrected QT) prolongation mediated by lapatinib was reversed by isoproterenol (an activator of I_{K_s}) in mice [27, 28], which may explain the more significant decrease in the rate observed with WT-hiPSC-CMs than with LQT-hiPSC-CMs, to a certain degree.

The stability of ion channels, ion carriers, and ion flow in CMs is essential for their efficient operation. Mutations in *KCNQ1* that cause LQT1 can reduce I_{K_s} and prolong action potential duration (APD) by two mechanisms: 1) impaired trafficking of KCNQ1 proteins to the plasma membrane and 2) dysfunction of membrane channel proteins [29]. The significantly decreased CI indicates that cytotoxicity caused by the “off-target effect” played an important role in the cardiotoxicity of TKIs. TKIs mainly modulate CM functions via various signaling pathways and mechanisms such as mitochondrial toxicity, inhibition of AMPK and PDGFR, and effects on the vasculature [2, 30–32].

The effect on electrical activity of CMs is the secondary cause of TKI-induced cardiotoxicity, and inhibition of certain ion channels might have severe detrimental effects in patients with congenital ion channel diseases. The APD of ventricular-like hiPSC-CMs derived from an LQT1 patient treated with ML277 was shortened significantly, and LQT1-specific CMs were more sensitive to the effect of I_{K_r} blockade than non-LQT1-specific CMs, which prolonged the QTc more significantly in the former cells [9, 33, 34]. This confirms the compensatory enhancement of I_{K_r} in LQT1 patients due to the lack of I_{K_s} , which indicates that drugs that block I_{K_r} have a higher risk of inducing arrhythmia in LQT1 patients than drugs that do not block this channel, similar to sunitinib.

In contrast, multichannel blockers probably do not exert a more potent effect on LQT1 patients than on non-LQT1 patients because of comprehensive physiological regulatory processes. In particular, similar to non-LQT1 patients, those with LQT1 might not develop arrhythmias caused by agents that block I_{K_s} , such as lapatinib. Moreover, the effect on sodium channels may indirectly affect intracellular calcium

concentrations via $\text{Na}^+ \text{-Ca}^{2+}$ exchange, leading to regulation of the sarcoplasmic reticulum Ca^{2+} load and effects on contractility.

In summary, crizotinib, sunitinib, and lapatinib were considered to have a high risk for affecting cardiac myocardial contraction, consistent with the findings of previous studies, whereas dasatinib was found to be relatively safe [35]. Moreover, LQT1 patients should be monitored when using sunitinib. The current study provides valuable information on the mechanisms by which TKIs affect cardiac myocardial contraction of both WT- and LQT-hiPSC-CMs. Because of the high throughput and accuracy of this current platform, it is expected to contribute to saving costs during drug screening and facilitating drug discovery pipelines. Patient-derived hiPSC-CMs simulate the characteristics of genetic cardiac diseases and, therefore, could facilitate clarification of the mechanisms involved in the development and progression of diseases caused by genetic factors. Furthermore, patient-derived hiPSC-CMs could be used to determine whether a patient's genetic composition would affect their likelihood of developing drug-induced cardiotoxicity. The results of this study also provide a reference for appropriate drug treatment with TKIs and their management.

The present study has some obvious limitations that are worth mentioning. The G219E mutation in the voltage-sensing domain of *KCNQ1* and the resulting pathogenic mechanisms have not been reported yet. The comparison of CMs derived from a healthy control donor and the patient did not account for potential gene polymorphisms. Finally, whether CMs carrying the G219E mutation in *KCNQ1* could reflect the responses of all LQT1 patients to the investigated TKIs still requires comprehensive verification.

Conclusion

In conclusion, we found that WT-hiPSC-CMs and LQT-hiPSC-CMs from different sources exhibited similar responses to several TKIs. To the best of our knowledge, this is the first such report. Of the four tested drugs, crizotinib, sunitinib, and lapatinib induced a higher degree of cardiotoxicity than dasatinib, which we considered to be a relatively safe and effective drug, as previously reported. Moreover, LQT1 patients should exercise extreme caution with sunitinib. Following exposure to the tested drugs, the healthy hiPSC- and LQT-hiPSC-CMs exhibited different outcomes involving their mechanical beating properties and varying sensitivities. These findings could contribute to providing a platform for precision medicine and drug screening in the future.

Abbreviations

ALK, anaplastic lymphoma kinase; **AMPK**, AMP-activated protein kinase; **APD**, action potential duration; **CI**, cell index; **ECG**, electrocardiogram; **EGFR**, epidermal growth factor receptor; **FDA**, US Food and Drug Administration; **CM**, cardiomyocyte; **CML**, chronic myeloid leukemia; **HER2**, human epidermal growth factor receptor 2; **hERG**, human ether-a-go-go-related gene; **hiPSC-CMs**, human induced pluripotent stem cell-derived cardiomyocytes; **IC₅₀**, half maximal inhibitory concentration; **I_{Ks}**, slow delayed rectifier current; **LVEF**, left ventricular ejection fraction; **LQT**, long QT syndrome; **MET**, MET protooncogene; **NSCLC**, non-

small cell lung cancer; **PDGF**, platelet-derived growth factor; **ROS**, reactive oxygen species; **ROS1**, c-fos oncogene1; **RTCA**, xCELLigence® real-time cell analysis; **VEGF**, vascular epidermal growth factor; **TdP**, torsade de pointes; **TKI**, tyrosine kinase inhibitor; **WT**, wild type

Declarations

Ethics approval and consent to participate

HiPSC-CMs were obtained from Beijing Cellapy Biotechnology Co., Ltd and Nanjing HELP Stem Cell Innovations Co., Ltd. For both cell types, informed consent was obtained from donors in compliance with all national regulations.

Consent for publication

Not applicable.

Availability of data and materials

The data that support the findings of this study are available from the corresponding author upon reasonable request.

Competing interests

The authors declare that they have no competing interests.

Funding

This study was supported by the National Foundation of Science and Technology (2018ZX09201017-008) and Shanghai Foundation of Science and Technology (17140900700).

Authors' contributions

XW and YZ designed the research. YZ performed the experiments. MW and HX prepared all figures. YZ wrote the main manuscript text. XW and QZ revised the manuscript text and figures and provided scientific suggestions. All authors analyzed the data, reviewed the manuscript, and read and approved the final manuscript.

Acknowledgements

We thank Cellapy and HELP for providing the stable hiPSC-CMs and Qi Zhao for supporting the study methods.

Authors' details

¹China State Institutes of Pharmaceutical Industry, Shanghai, China. ² Shanghai InnoStar Bio-Tech Co., Ltd.

References

1. Zarifa A, Albittar A, Kim PY, Hassan S, Palaskas N, Iliescu C, et al. Cardiac toxicities of anticancer treatments: chemotherapy, targeted therapy and immunotherapy. *Curr Opin Cardiol.* 2019;34:441–50.
2. Mellor HR, Bell AR, Valentin JP, Roberts RR. Cardiotoxicity associated with targeting kinase pathways in cancer. *Toxicol Sci.* 2011;120:14–32.
3. Sethi TK, Basdag B, Bhatia N, Moslehi J, Reddy NM. Beyond Anthracyclines: Preemptive Management of Cardiovascular Toxicity in the Era of Targeted Agents for Hematologic Malignancies. *Curr Hematol Malig Rep.* 2017;12:257–67.
4. Pourrier M, Fedida D. The Emergence of Human Induced Pluripotent Stem Cell-Derived Cardiomyocytes (hiPSC-CMs) as a Platform to Model Arrhythmogenic Diseases. *Int J Mol Sci.* 2020;21:E657.
5. Brodehl A, Ebbinghaus H, Deutsch MA, Gummert J, Gartner A, Ratnavadivel S, et al. Human Induced Pluripotent Stem-Cell-Derived Cardiomyocytes as Models for Genetic Cardiomyopathies. *Int J Mol Sci.* 2019;20:E4381.
6. Yang B, Papoian T. Preclinical approaches to assess potential kinase inhibitor-induced cardiac toxicity: Past, present and future. *J Appl Toxicol.* 2018;38:790–800.
7. Magdy T, Schuldt AJT, Wu JC, Bernstein D, Burridge PW. Human Induced Pluripotent Stem Cell (hiPSC)-Derived Cells to Assess Drug Cardiotoxicity: Opportunities and Problems. *Annu Rev Pharmacol Toxicol.* 2018;58:83–103.
8. Gintant G, Burridge P, Gepstein L, Harding S, Herron T, Hong C, et al. Use of Human Induced Pluripotent Stem Cell-Derived Cardiomyocytes in Preclinical Cancer Drug Cardiotoxicity Testing: A Scientific Statement From the American Heart Association. *Circ Res.* 2019;125:e75–92.
9. Ma D, Wei H, Lu J, Huang D, Liu Z, Loh LJ, et al. Characterization of a novel KCNQ1 mutation for type 1 long QT syndrome and assessment of the therapeutic potential of a novel IKs activator using patient-specific induced pluripotent stem cell-derived cardiomyocytes. *Stem Cell Res Ther.* 2015;6:39.
10. Kuusela J, Kujala VJ, Kiviahko A, Ojala M, Swan H, Kontula K, et al. Effects of cardioactive drugs on human induced pluripotent stem cell derived long QT syndrome cardiomyocytes. *Springerplus.* 2016;5:234.
11. Tseng GN. Structure-function relationship of the slow delayed rectifier channel: impactful questions in 2020 and beyond. *Am J Physiol Heart Circ Physiol.* 2020;318:H329-31.
12. Wu J, Ding W-G, Horie M. Molecular pathogenesis of long QT syndrome type 1. *J Arrhythm.* 2016;32:381–8.
13. Zhao Q, Wang X, Wang S, Song Z, Wang J, Ma J. Cardiotoxicity evaluation using human embryonic stem cells and induced pluripotent stem cell-derived cardiomyocytes. *Stem Cell Res Ther.* 2017;8:54.

14. Paci M, Hyttinen J, Aalto-Setala K, Severi S. Computational models of ventricular- and atrial-like human induced pluripotent stem cell derived cardiomyocytes. *Ann Biomed Eng.* 2013;41:2334–48.
15. Paci M, Casini S, Bellin M, Hyttinen J, Severi S. Large-Scale Simulation of the Phenotypical Variability Induced by Loss-of-Function Long QT Mutations in Human Induced Pluripotent Stem Cell Cardiomyocytes. *Int J Mol Sci.* 2018;19:3583.
16. Oyakawa T, Muraoka N, Iida K, Kusuhara M, Kawamura T, Naito T, et al. Crizotinib-induced simultaneous multiple cardiac toxicities. *Invest New Drug.* 2018;36:949–51.
17. Tartarone A, Gallucci G, Lazzari C, Lerose R, Lombardi L, Aieta M. Crizotinib-induced cardiotoxicity: the importance of a proactive monitoring and management. *Future Oncol.* 2015;11:2043–8.
18. Doherty KR, Wappel RL, Talbert DR, Trusk PB, Moran DM, Kramer JW, et al. Multi-parameter in vitro toxicity testing of crizotinib, sunitinib, erlotinib, and nilotinib in human cardiomyocytes. *Toxicol Appl Pharmacol.* 2013;272:245–55.
19. Gallucci G, Tartarone A, Lombardi L, Aieta M. When crizotinib-induced bradycardia becomes symptomatic: role of concomitant drugs. *Expert Rev Anticancer Ther.* 2015;15:761–3.
20. Ou SH, Tong WP, Azada M, Siwak-Tapp C, Dy J, Stiber JA. Heart rate decrease during crizotinib treatment and potential correlation to clinical response. *Cancer.* 2013;119:1969–75.
21. Yang Y, Bu P. Progress on the cardiotoxicity of sunitinib: Prognostic significance, mechanism and protective therapies. *Chem Biol Interact.* 2016;257:125–31.
22. Damrongwatanasuk R, Fradley MG. Cardiovascular Complications of Targeted Therapies for Chronic Myeloid Leukemia. *Curr Treat Options Cardiovasc Med.* 2017;19:24.
23. Hasinoff BB, Patel D. Mechanisms of the Cardiac Myocyte-Damaging Effects of Dasatinib. *Cardiovasc Toxicol.* 2020. doi:10.1007/s12012-020-09565-7.
24. Izumi-Nakaseko H, Fujiyoshi M, Hagiwara-Nagasawa M, Goto A, Chiba K, Kambayashi R, et al. Dasatinib can Impair Left Ventricular Mechanical Function But May Lack Proarrhythmic Effect: A Proposal of Non-clinical Guidance for Predicting Clinical Cardiovascular Adverse Events of Tyrosine Kinase Inhibitors. *Cardiovasc Toxicol.* 2020;20:58–70.
25. Choi HD, Chang MJ. Cardiac toxicities of lapatinib in patients with breast cancer and other HER2-positive cancers: a meta-analysis. *Breast Cancer Res Treat.* 2017;166:927–36.
26. Jerusalem G, Lancellotti P, Kim SB. HER2 + breast cancer treatment and cardiotoxicity: monitoring and management. *Breast Cancer Res Treat.* 2019;177:237–50.
27. Lee HA, Kim EJ, Hyun SA, Park SG, Kim KS. Electrophysiological effects of the anti-cancer drug lapatinib on cardiac repolarization. *Basic Clin Pharmacol Toxicol.* 2010;107:614–8.
28. Chang WT, Liu PY, Lee K, Feng YH, Wu SN. Differential Inhibitory Actions of Multitargeted Tyrosine Kinase Inhibitors on Different Ionic Current Types in Cardiomyocytes. *Int J Mol Sci.* 2020;21:E1672.
29. Sogo T, Morikawa K, Kurata Y, Li P, Ichinose T, Yuasa S, et al. Electrophysiological properties of iPS cell-derived cardiomyocytes from a patient with long QT syndrome type 1 harboring the novel mutation M437V of KCNQ1. *Regen Ther.* 2016;4:9–17.

30. Lankhorst S, Kappers MH, van Esch JH, Danser AH, van den Meiracker AH. Mechanism of hypertension and proteinuria during angiogenesis inhibition: evolving role of endothelin-1. *J Hypertens.* 2013;31:444–54. discussion 54.
31. Force T, Krause DS, Van Etten RA. Molecular mechanisms of cardiotoxicity of tyrosine kinase inhibition. *Nat Rev Cancer.* 2007;7:332–44.
32. Lage R, Dieguez C, Vidal-Puig A, Lopez M. AMPK: a metabolic gauge regulating whole-body energy homeostasis. *Trends Mol Med.* 2008;14:539–49.
33. Kiviah AL, Ahola A, Larsson K, Penttinen K, Swan H, Pekkanen-Mattila M, et al. Distinct electrophysiological and mechanical beating phenotypes of long QT syndrome type 1-specific cardiomyocytes carrying different mutations. *Int J Cardiol Heart Vasc.* 2015;8:19–31.
34. Egashira T, Yuasa S, Suzuki T, Aizawa Y, Yamakawa H, Matsuhashi T, et al. Disease characterization using LQTS-specific induced pluripotent stem cells. *Cardiovasc Res.* 2012;95:419–29.
35. Sharma A, Burridge PW, McKeithan WL, Serrano R, Shukla P, Sayed N, et al. High-throughput screening of tyrosine kinase inhibitor cardiotoxicity with human induced pluripotent stem cells. *Sci Transl Med.* 2017;9:eaaf2584.

Figures

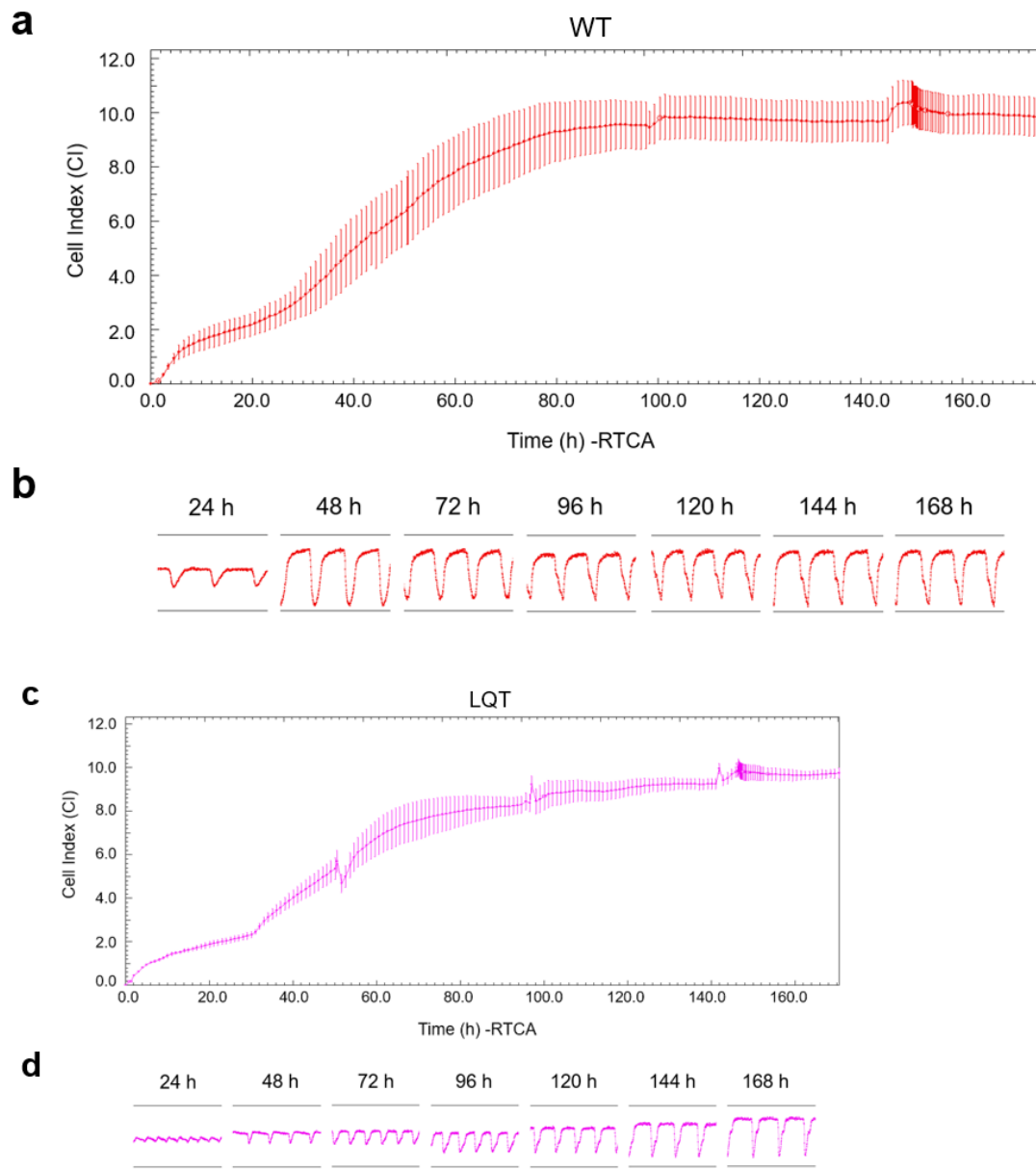
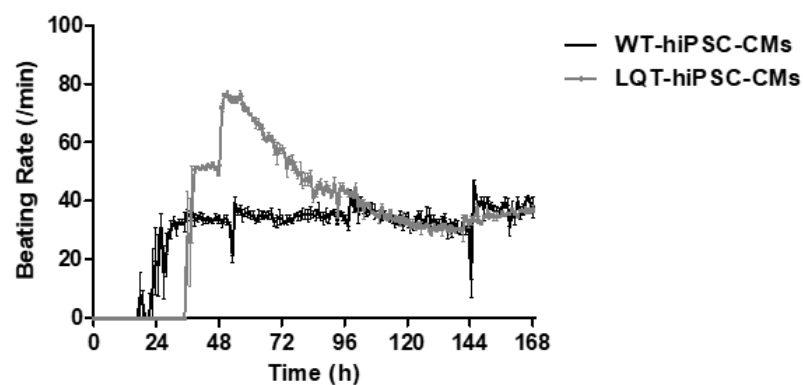
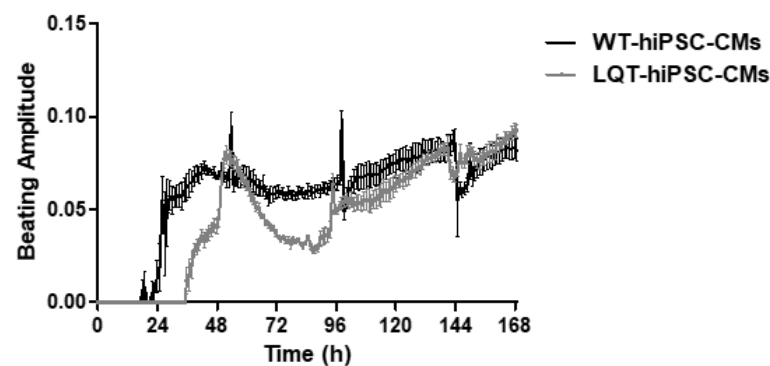
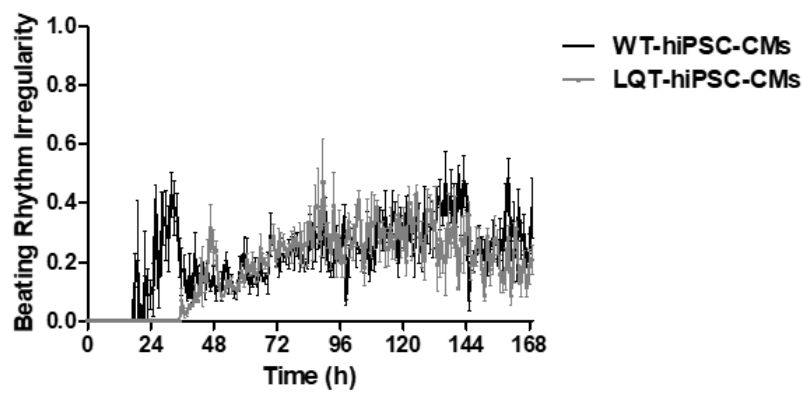


Figure 1

Growth and transient pulse patterns of human induced pluripotent stem cell-derived cardiomyocytes (a) Growth curve and (b) transient pulse patterns of wild-type human induced pluripotent stem cell-derived cardiomyocytes (WT-hiPSC-CMs). (c) Growth curve and (d) transient pulse patterns of long QT syndrome (LQT)-hiPSC-CMs. Data are means \pm standard error of the mean (SEM), n = 4.

a**b****c****Figure 2**

Relationship between beating (a) rate, (b) amplitude, and (c) rhythm irregularity of human induced pluripotent stem cell-derived cardiomyocytes (hiPSC-CMs) versus time cultured for 168 h. Data are means \pm standard error of the mean (SEM), n = 4.

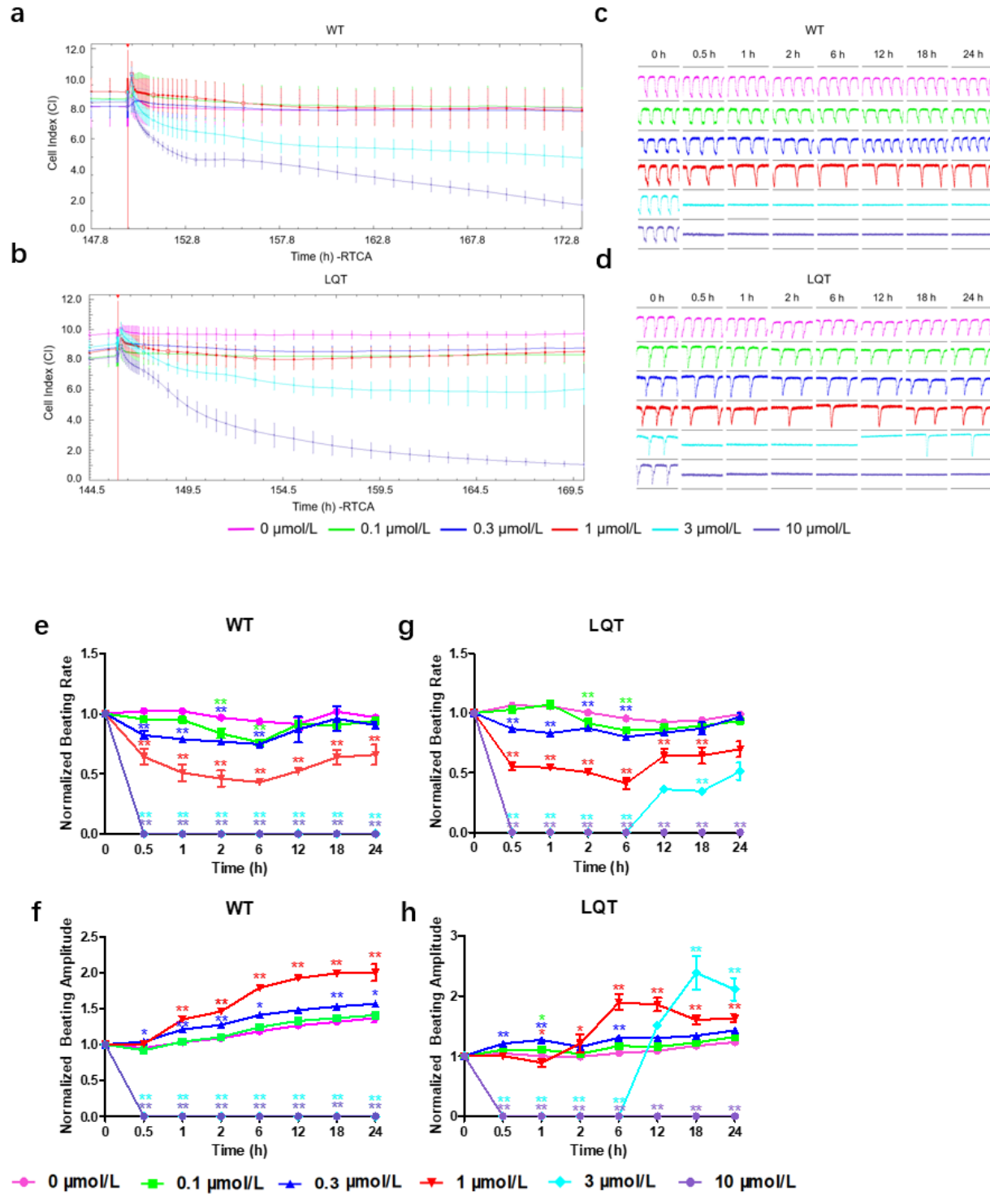


Figure 3

Effect of crizotinib on wild-type (WT)- and long QT syndrome (LQT)-human induced pluripotent stem cell-derived cardiomyocytes (hiPSC-CMs). Effect of crizotinib on cell index (CI) of (a) WT-hiPSC-CMs and (b) LQT-hiPSC-CMs. Effect of crizotinib on transient pulse patterns of (c) WT-hiPSC-CMs and (d) LQT-hiPSC-CMs. Effect of crizotinib on beating (e) rate and (f) amplitude of WT-hiPSC-CMs. Effect of crizotinib on

beating (g) rate and (h) amplitude of LQT-hiPSC-CMs. Data are means \pm standard error of the mean (SEM) of $n = 3\text{--}6$ experiments. * $p < 0.05$ and ** $p < 0.01$ compared to control. DMSO, dimethyl sulfoxide.

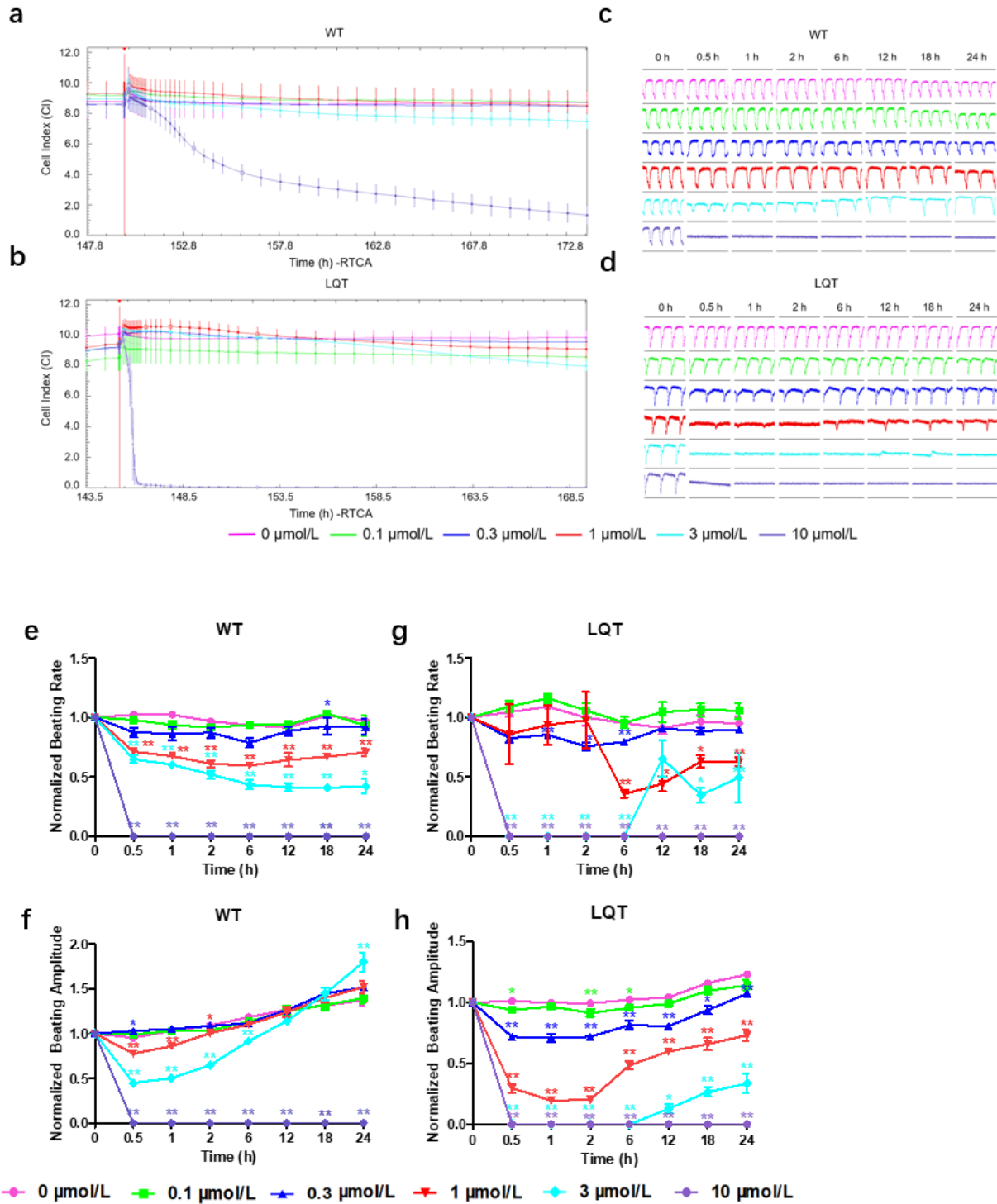


Figure 4

Effect of sunitinib on wild-type (WT)- and long QT syndrome (LQT)-human induced pluripotent stem cell-derived cardiomyocytes (hiPSC-CMs). Effect of sunitinib on cell index (CI) of (a) WT-hiPSC-CMs and (b) LQT-hiPSC-CMs. Effect of sunitinib on transient pulse patterns of (c) WT-hiPSC-CMs and (d) LQT-hiPSC-

CMs. Effect of sunitinib on beating (e) rate and (f) amplitude of WT-hiPSC-CMs. Effect of sunitinib on beating (g) rate and (h) amplitude of LQT-hiPSC-CMs. Data are means \pm standard error of the mean (SEM) of $n = 3\text{--}6$ experiments. * $p < 0.05$ and ** $p < 0.01$ compared to control.

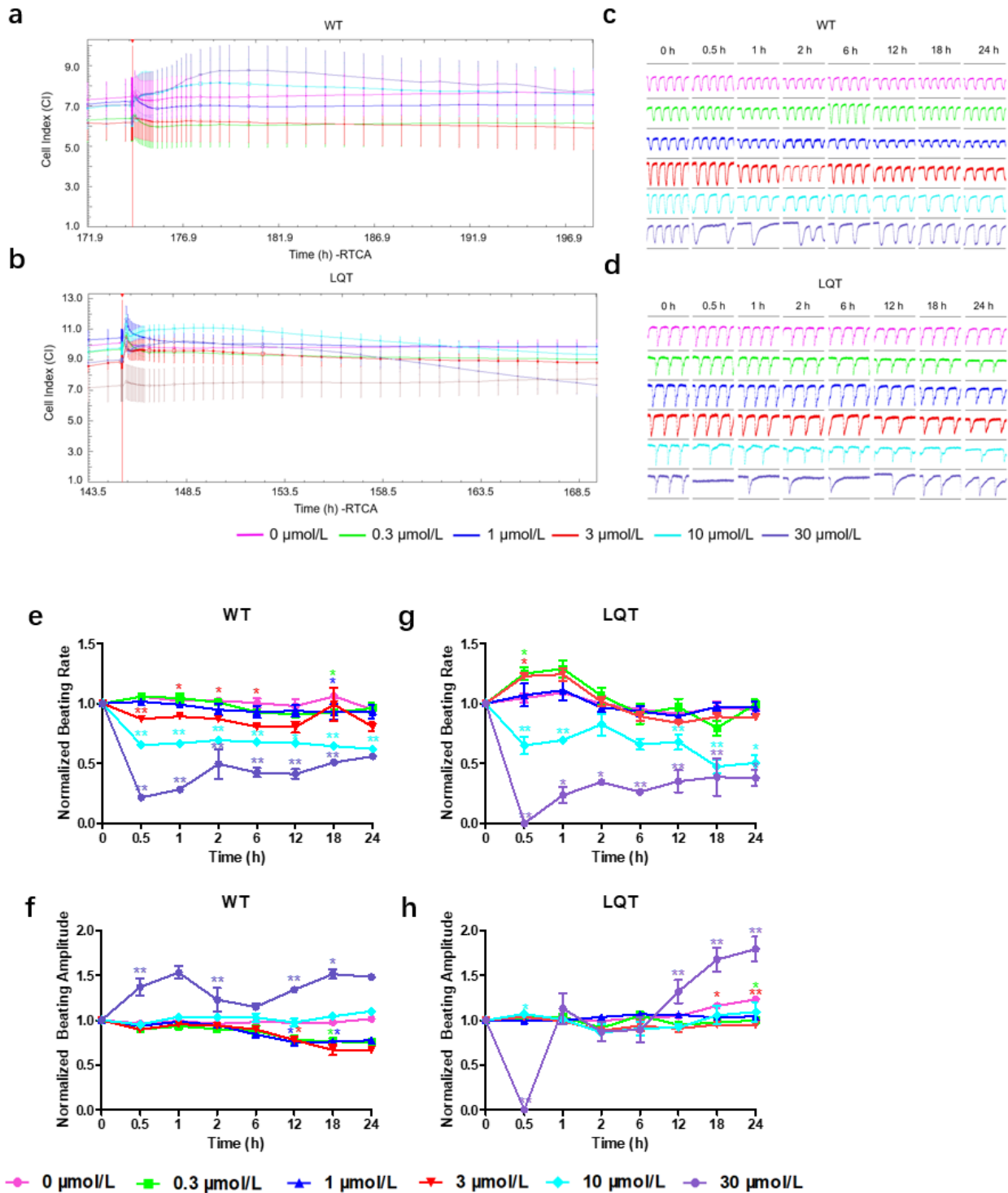


Figure 5

Effect of dasatinib on wild-type (WT)- and long QT syndrome (LQT)-human induced pluripotent stem cell-derived cardiomyocytes (hiPSC-CMs). Effect of dasatinib on cell index (CI) of (a) WT-hiPSC-CMs and (b)

LQT-hiPSC-CMs. Effect of dasatinib on transient pulse patterns of (c) WT-hiPSC-CMs and (d) LQT-hiPSC-CMs. Effect of dasatinib on beating (e) rate and (f) amplitude of the WT-hiPSC-CMs. Effect of dasatinib on beating (g) rate and (h) amplitude of LQT-hiPSC-CMs. Data are means \pm standard error of the mean (SEM) from $n = 3\text{--}6$ experiments. * $p < 0.05$ and ** $p < 0.01$ compared to control.

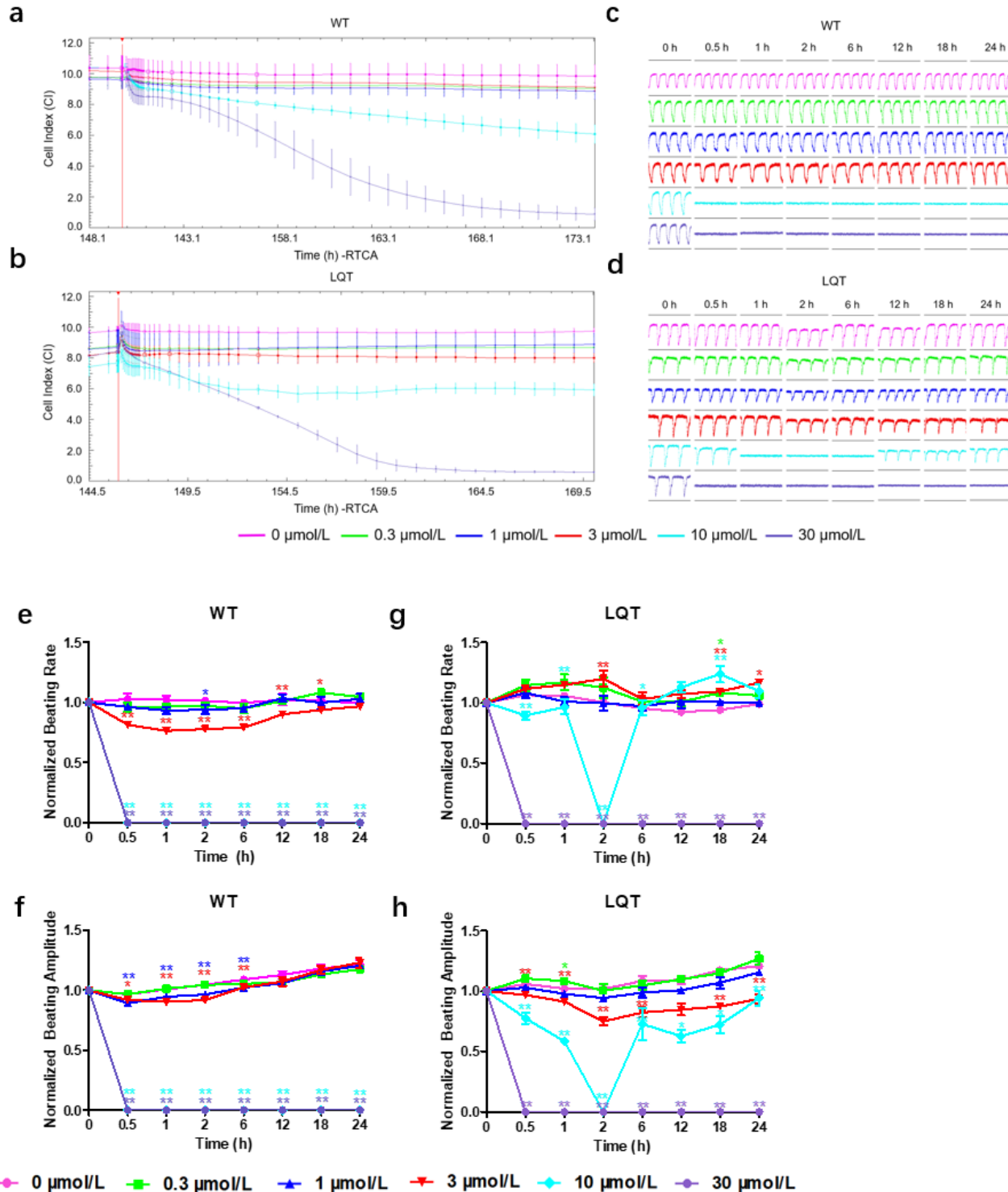


Figure 6

Effect of lapatinib on wild-type (WT)- and long QT syndrome (LQT)-human induced pluripotent stem cell-derived cardiomyocytes (hiPSC-CMs). Effect of lapatinib on cell index (CI) of (a) WT-hiPSC-CMs and (b) LQT-hiPSC-CMs. Effect of lapatinib on transient pulse patterns of (c) WT-hiPSC-CMs and (d) LQT-hiPSC-CMs. Effect of lapatinib on beating (e) rate and (f) amplitude of WT-hiPSC-CMs. Effect of lapatinib on beating (g) rate and (h) amplitude of LQT-hiPSC-CMs. Data are means ± standard error of the mean (SEM) of n =4–7 experiments. *p < 0.05 and **p < 0.01 compared to control.